Progress In Electromagnetics Research, PIER 81, 447–459, 2008

APPLICATION OF SVD NOISE-REDUCTION TECHNIQUE TO PCA BASED RADAR TARGET RECOGNITION

K.-C. Lee, J.-S. Ou, and M.-C. Fang

Department of Systems and Naval Mechatronic Engineering
National Cheng-Kung University
Tainan 701, Taiwan

Abstract—The noise effect is very challenging in radar target recognition. It usually degrades the accuracy of target recognition and then makes the recognition unreliable. In this study, we present a noise-reduction technique to improve the accuracy of radar target recognition. Our noise-reduction technique is based on the SVD (singular value decomposition). The PCA (principal components analysis) based radar recognition algorithm is utilized to verify our noise-reduction scheme. In our treatment, the received signals are arranged into a Hankel-form matrix. This Hankel-form matrix is decomposed into two subspaces, i.e., the noise-related subspace and clean-signal subspace. The noise reduction is obtained by suppressing the noise-related subspace and retaining the clean-signal space only. Simulation results show that the accuracy of target recognition is greatly improved as the received signals are first processed by the SVD noise-reduction technique. With the use of proposed noise-reduction scheme, the radar target recognition can tolerate more noises and then becomes more reliable. The noise-reduction technique in this study can also be applied to many other problems in radar engineering.

1. INTRODUCTION

Radar target recognition [1–3] means to identify targets or achieve the fundamental information of targets by received electromagnetic signals. In practical measurement, the received signals contain a lot of random noises in addition to the clean signals. These random noises may destroy the recognition and then make the recognition unreliable. In other words, the noise effects are very challenging in radar target recognition. This then motivates us to develop an efficient and powerful noise-reduction scheme to improve the accuracy of radar target recognition.

In this paper, we present a noise-reduction scheme to improve the accuracy of radar target recognition. Our noise-reduction technique is based on the SVD (singular value decomposition) [4]. In our treatment, the received signals are arranged into a Hankel-form matrix. This Hankel-form matrix is decomposed into two subspaces, i.e., the noise-related subspace and clean-signal subspace. The noise reduction is obtained by suppressing the noise-related subspace and retaining the clean-signal space only.

After the received electromagnetic signals have been processed by the above noise-reduction technique, the resulting signals are nearly clean. These nearly clean signals are then utilized for radar target recognition. In this study, the PCA (principal components analysis) [5] and angular-diversity based radar target recognition algorithm [6] is utilized to verify our SVD noise-reduction scheme. Simulation results show that the accuracy of target recognition is greatly improved as the received signals are first processed by our noise-reduction scheme. The SVD based concept has been utilized in speech [7, 8] and imaging [9] signal processing. However, there is still no research that applies such a noise-reduction technique to radar target recognition. To our knowledge, this is the first study that applies SVD noise-reduction technique to such a problem. With the use of proposed noise-reduction scheme, the radar target recognition can tolerate more noises and then becomes more reliable.

In Section 2, the theoretical formulations are given. Numerical simulation results are given in Section 3. Finally, the conclusion is given in Section 4.

2. FORMULATIONS

Without loss of generality, we consider a ship on the sea level (X-Y plane) located at the origin of coordinate for simplicity, as shown in Figure 1. Note that this study has no limitation in types of targets. In Figure 1, the front end of ship is in the $+\hat{x}$ direction and the broadside of ship is in the $\pm\hat{y}$ direction. The spherical coordinate system is defined as (R, θ, ϕ) where R is the distance from observation position to origin, θ is the elevation angle and ϕ is the azimuth angle. The ship is illuminated by a plane wave $\overline{E}_i = e^{+jk_0x}\hat{z}$ where k_0 is the wavenumber. The bistatic RCS (radar cross section) in the direction

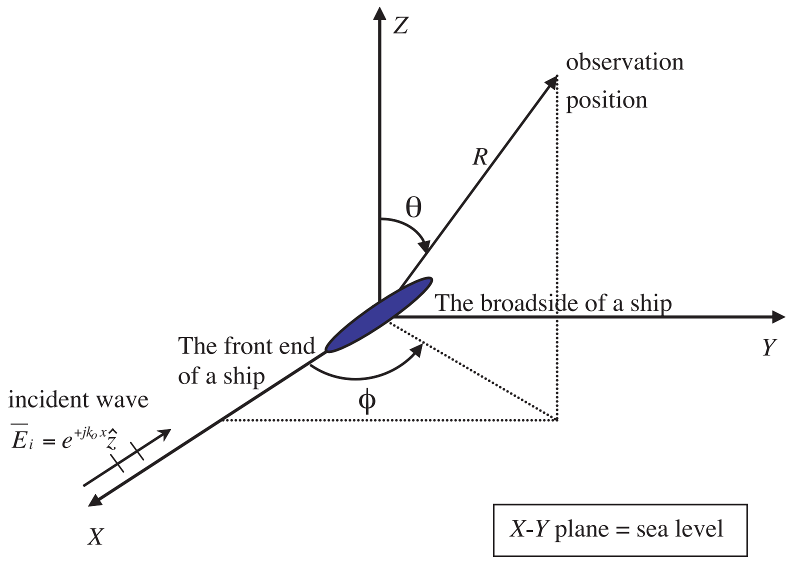

Figure 1. Schematic diagram of a ship illuminated by an incident plane wave.

of (θ, ϕ) is defined as [10]

$$\sigma(\theta, \phi) = \lim_{R\to\infty} 4\pi R^2 \frac{\left|\overline{E}_s(\theta, \phi)\right|^2}{\left|\overline{E}_i\right|^2}. \tag{1}$$

where $\overline{E}_s(\theta, \phi)$ is the scattered electric field. The bistatic RCS of a ship at a fixed elevation angle θ and different N azimuth angles of ϕ are collected to constitute an RCS vector $\overline{u} = [\ u_1 \quad u_2 \quad \cdots \quad u_N\ ]^T$, where "$T$" denotes the transpose.

In practical measurement, the collected RCS $\overline{u}$ contains a lot of noises. In this study, the measured $\overline{u}$ is processed by the SVD technique [4] to reduce the noise. In general, the noisy $\overline{u}$ consists of the clean signal $\overline{v} = [\ v_1 \quad v_2 \quad \cdots \quad v_N\ ]^T$ and the addition noise $\overline{n} = [\ n_1 \quad n_2 \quad \cdots \quad n_N\ ]^T$, i.e.,

$$\overline{u} = \overline{v} + \overline{n}. \tag{2}$$

In (2), $\overline{v}$ is deterministic and $\overline{n}$ is random. The goal is to extract the clean $\overline{v}$ from the noisy $\overline{u}$. To achieve this goal, the subspace concept is utilized for noise reduction and a Hankel-form matrix is defined as

$$\overline{\overline{H}}_u = \begin{bmatrix} u_1 & u_2 & \cdots & u_J \\ u_2 & u_3 & \cdots & u_{J+1} \\ \vdots & \vdots & & \vdots \\ u_I & u_{I+1} & \cdots & u_{I+J-1} \end{bmatrix}_{I\times J} . \tag{3}$$

The dimension of $\overline{\overline{H}}_u$ is $I \times J$, where $I + J = N + 1$ and $I \geq J$. From (2)–(3), the noisy $\overline{\overline{H}}_u$ can be represented as the summation of two Hankel-form matrices as

$$\overline{\overline{H}}_u = \overline{\overline{H}}_v + \overline{\overline{H}}_n, \tag{4}$$

where $\overline{\overline{H}}_v$ and $\overline{\overline{H}}_n$ represents the contributions from clean signals and random noises, respectively. The structures of $\overline{\overline{H}}_v$ and $\overline{\overline{H}}_n$ are similar to (3) except that u_i $(i = 1, 2, \ \ldots, I + J - 1)$ is replaced by v_i and n_i, respectively. The clean signal $\overline{v}$ can be successfully extracted as $\overline{\overline{H}}_v$ is obtained. By using the SVD technique, we can decompose the matrix $\overline{\overline{H}}_u$ into

$$\overline{\overline{H}}_u = \overline{\overline{L}}\,\overline{\overline{\Sigma}}\,\overline{\overline{R}}^T . \tag{5}$$

In (5), the columns of $\overline{\overline{L}}$ (dimension $I \times I$) and $\overline{\overline{R}}$ (dimension $J \times J$) are called left and right singular vectors, respectively. All of these column vectors are orthogonal. The matrix $\overline{\overline{\Sigma}}$ is diagonal with dimension $I\times J$ and is defined as $\overline{\overline{\Sigma}} = diag\{s_1, s_2, \cdots, s_{Min(I,J)}\}$, where s_i $(i = 1, 2, \ldots, Min(I, J))$ is the singular value and $s_1 \geq s_2 \ldots \geq s_{Min(I,J)} \geq 0$. Physically, the largest singular value contributes almost only clean signal information, whereas the smallest singular value contributes almost only noise information. To extract the clean signal, the largest K singular values are viewed as the clean components. The remaining $Min(I, J) - K$ singular values are viewed as the noise components and are discarded. Therefore, the noise reduction can be obtained by adjusting the singular values as

$$\overline{\overline{\Sigma'}} = \begin{bmatrix} s_1 & 0 & \cdots & 0 & 0 & \cdots \\ 0 & s_2 & \vdots & \vdots & 0 & \cdots \\ \vdots & \vdots & \ddots & 0 & 0 & \cdots \\ 0 & \cdots & 0 & s_K & 0 & \cdots \\ 0 & \cdots & 0 & 0 & 0 & \cdots \\ 0 & \cdots & \cdots & \cdots & \cdots & \ddots \end{bmatrix}_{I\times J} . \tag{6}$$

A new matrix $\overline{\overline{H}}_{v'}$ is then constructed as

$$\overline{\overline{H}}_{v'} = \overline{\overline{L}}\,\overline{\overline{\Sigma'}}\,\overline{\overline{R}}^T \tag{7}$$

to approximate the clean contribution. Note that $\overline{\overline{H}}_{v'}$ in (7) is no longer Hankel-form. In our treatment, the anti-diagonal components of $\overline{\overline{H}}_{v'}$ are averaged to generate the modified $\overline{\overline{H}}_{v'}$ and the resulting matrix will be Hankel-form. The estimation of the clean signal $\overline{v}$ is denoted as $\overline{v'}$ and will be reconstructed from the modified $\overline{\overline{H}}_{v'}$. In other words, $\overline{v'}$ is the approximation for the clean signal $\overline{v}$. Conventional radar recognition utilized the noisy signal $\overline{u}$ for target identification, whereas we utilized the nearly clean signal $\overline{v'}$ for target identification.

In this study, the PCA and angular-diversity based radar target recognition algorithm [6] is utilized to verify our SVD noise-reduction scheme. The recognition procedures are given in [6] and the results are given in the following section.

3. NUMERICAL SIMULATION RESULTS

In this section, numerical examples are given to verify our noise-reduction scheme in radar target recognition. Note that our noise-reduction scheme has no limitation in types of targets. To easily obtain the RCS data by simulation, simplified ship models are utilized instead of real ships. Assume there are three types of known ships ($P = 3$) including type I (to model the container vessel), type II (to model the naval ship) and type III (to model the fishing boat). The geometrical models for the three types of known ships are shown in Figure 2. The ship length l is chosen to be $k_0 l = 9.4$ for the ship of type I, $k_0 l = 6.3$ for the ship of type II, and $k_0 l = 3.1$ for the ship of type III. All ships are on rough sea surface (X-Y plane). The characteristic for surface roughness of sea water is assumed to be

$$z(x, y) = \frac{4}{75} l \cdot \sin\left(\frac{15\pi}{4} x\right) \sin\left(\frac{15\pi}{4} y\right) + \frac{8}{75} l. \tag{8}$$

The sea water has dielectric constant 81 and conductivity 4 S/m. In the simulation of RCS, the commercial software Ansoft HFSS is exploited. This software was proved to be accurate by many researchers in this field. As the arrangement in Figure 1, the bistatic RCS from each type of known ship at a fixed elevation angle θ and 181 (i.e., $N = 181$) azimuth angles of $\phi = 0°, 1°, \ldots, 180°$ are calculated by Ansoft HFSS software. To model the practical measurement including

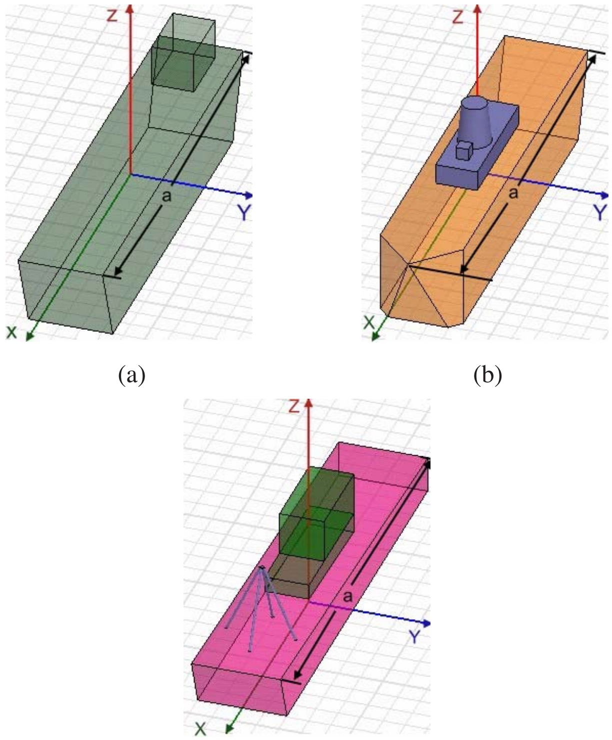

(a) (b) (c)

Figure 2. Geometrical models for three known classes of ships: (a) type I, (b) type II and (c) type III.

random noises, we add to each RCS a quantity of independent random noise having a Gaussian distribution with zero mean. The standard derivation of noise is 4×10^{-1} normalized with respect to the root-mean square value of the RCS. This noisy RCS vector $\overline{u}_i$ is first processed by the SVD noise-reduction scheme and the result is $\overline{v'}_i$ (nearly clean). In the SVD, the dimension of the Hankel-form matrix is $I = 91$ and $J = 91$. The number of reserved singular values in (6) is chosen as $K = 15$, i.e., the remaining 76 singular values are discarded. This implies that the largest 15 singular values are viewed as contribution of clean signals and the remaining 76 singular values are viewed as contribution of noises. The choice for the number of reserved singular values depends on experiences. By sampling the elevation angles at $\theta = 61°$, $63°$, ... , $89°$, we have $M_1 = M_2 = M_3 = 15$ and $M = 45$. The number of principal components in the PCA recognition is chosen to be $M' = 2$.

Initially, the projected features of training RCS data in Step-1 are given. Figure 3 shows the projected features on the 2-dimensional PCA space for the training RCS data of the three known ships. In Figure 3(a), the noisy RCS data are not processed by any noise-reduction scheme. From Figure 3(a), it shows that projected features of type I and type II distribute close together. As the noisy RCS data are first processed by our SVD noise-reduction scheme, the projected features of all the three classes are well separated and are shown in Figure 3(b). This example convinces us that the SVD based noise-reduction scheme can really improve the target recognition. From Figure 3, it shows there may be confusion in identifying the targets of type I and type II. Therefore, we give further testing for these two types of targets.

In the first testing, we assumed that the unknown target is just the target of type I. The testing is implemented 15 times at $\theta = 62°$, $64°$, $\ldots$, $90°$, respectively. It should be noted that these testing elevation angles are different from those for collecting the training data in Step-1. Figure 4 shows the distance to feature centers (i.e., class error) for the three known classes of ship RCS under 15 testing elevation angles at $\theta = 62°$, $64°$, $\ldots$, $90°$, respectively. According to [6], the magnitude of distance (class error) is in inverse proportion to the degree of similarity. The smallest distance (class error) means that the target ship has the highest degree of similarity with the corresponding type of ship. Therefore, the lowest plot line represents the prediction for the unknown target (should be type I in this example), because this plot line has the shortest distance (to the unknown target) among the three known targets. In Figure 4(a), the noisy RCS data are not processed by any noise-reduction scheme. From Figure 4(a), it shows that the lowest two plots (for type I and type II) distribute close together. One may be confused in identifying the two targets. As the noisy RCS data are first processed by our SVD noise-reduction scheme, the distance (i.e., class error) is shown in Figure 4(b). From Figure 4(b), it shows that the lowest two plots (for type I and type II) are well separated.

In the second testing, we assumed that the tested target is just the target of type II. The remaining procedures are the same as those of the previous example. Figure 5 shows the distance to feature centers (i.e., class error) for the three known classes of ship RCS under 15 testing elevation angles respectively. The lowest plot line is expected to be type II in this example. In Figure 5(a), the noisy RCS data are not processed by any noise-reduction scheme. From Figure 5(a), it shows that the lowest two plots (for type I and type II) distribute close together. One may be confused in identifying the two targets. As the noisy RCS data

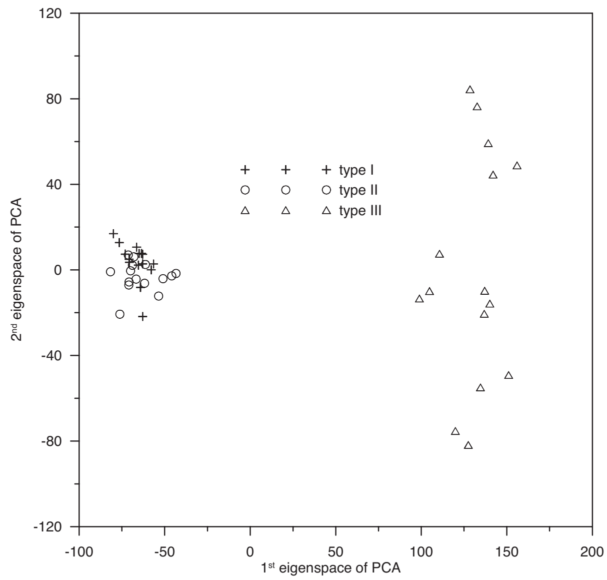

(a)

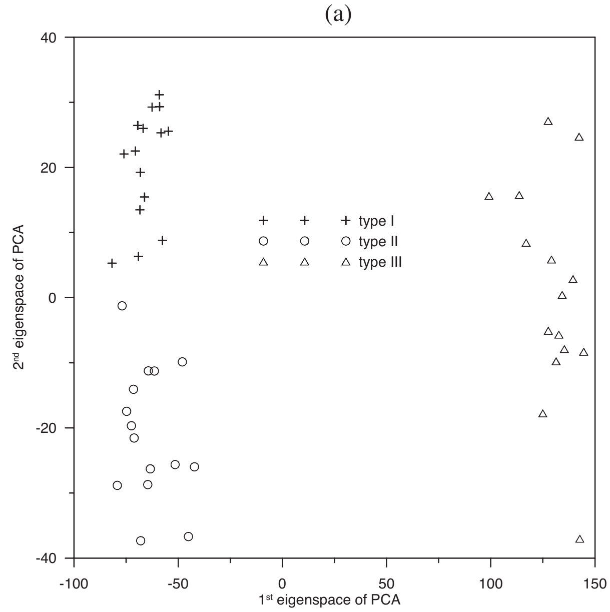

(b)

Figure 3. The projected features on the 2-dimensional PCA space for the training RCS data of the three known ships: (a) without any noise-reduction processing, and (b) with SVD noise-reduction processing.

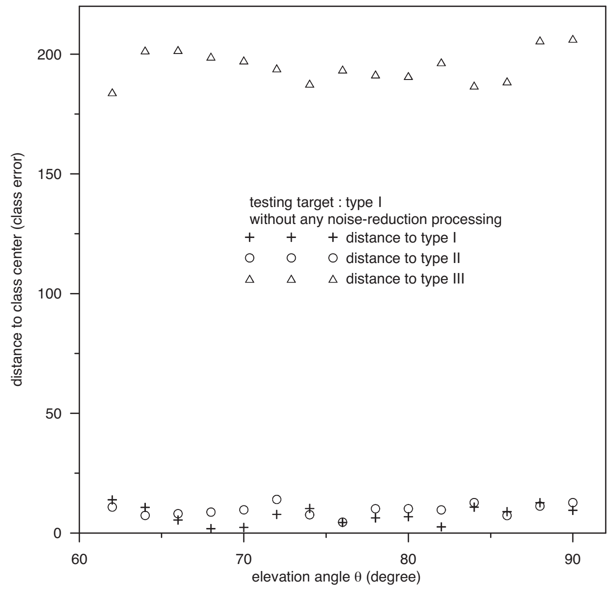

(a)

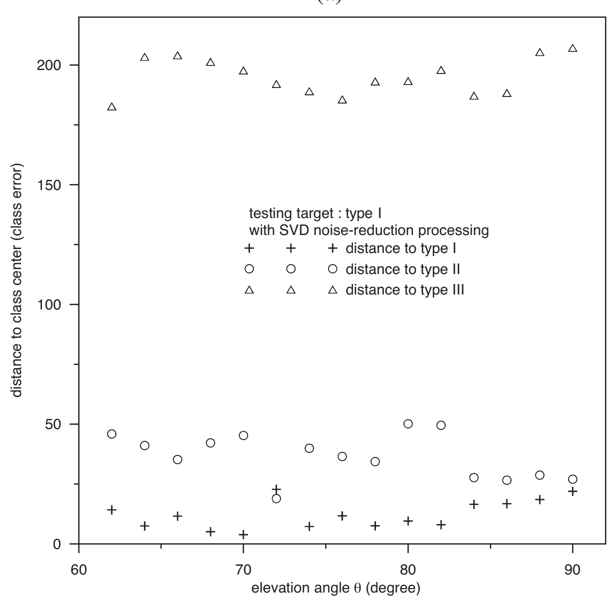

(b)

Figure 4. The distance (i.e., class error) to feature centers for the three known classes of ship RCS at different elevation angles θ by using ship of type I as the testing target: (a) without any noise-reduction processing, and (b) with SVD noise-reduction processing.

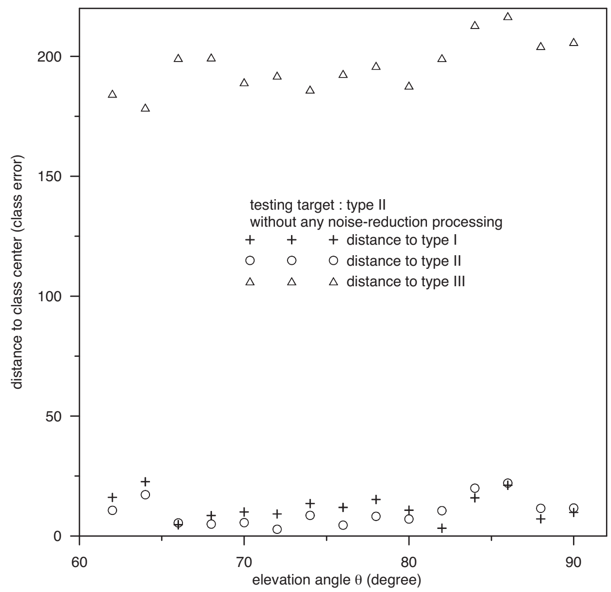

(a)

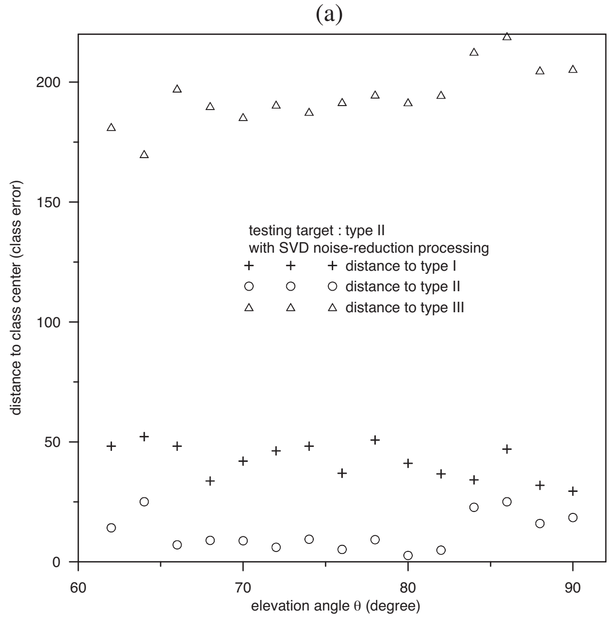

(b)

Figure 5. The distance (i.e., class error) to feature centers for the three known classes of ship RCS at different elevation angles θ by using ship of type II as the testing target: (a) without any noise-reduction processing, and (b) with SVD noise-reduction processing.

are first processed by our SVD noise-reduction scheme, the distance (i.e., class error) is shown in Figure 5(b). From Figure 5(b), it shows that the lowest two plots (for type I and type II) are well separated. The results of the above two examples convince us that the SVD noise-reduction scheme can improve the target recognition.

The above results of RCS data are calculated on a personal computer with Pentium-3.0 CPU. The signal-processing programs are coded using the Matlab-7 software.

4. CONCLUSIONS

The random noises of measured electromagnetic signals are challenging problems in radar target recognition. In this paper, a noise-reduction scheme based on SVD is proposed to treat the PCA radar target recognition. In noise-reduction procedures, the subspace concepts are utilized, i.e., suppressing the noise-related subspace and reserving only the clean-signal subspace. Simulation results show that the recognition accuracy is greatly improved as the RCS data are fist processed by the SVD noise-reduction scheme. With the use of our noise-reduction scheme, the target recognition can tolerate random noises and then its results become more reliable. The models of targets in this study are somewhat simple. However, this is not important because our main purpose is to illustrate that the SVD-based noise-reduction scheme can reduce the noise effects in target recognition. From physical points of view, only the clean signal can give information of the target. Therefore, noise-reduction processing on collected data becomes necessary. This study can be applied to many other applications in radar target recognition [11–21].

ACKNOWLEDGMENT

The work in this paper was supported by the National Science Council, Taiwan, under Grant NSC NSC 96-2628-E-006-250-MY3, and by the Landmark Program for NCKU's Top-University Project under grant 96-B041. The author would like to express his sincere gratitude to them.

REFERENCES

1. Hajduch G., J. M. Le Caillec, and R. Garello, "Airborne high-resolution ISAR imaging of ship targets at sea," *IEEE Transactions on Aerospace and Electronic Systems*, Vol. 40, No. 1, 378–384, 2004.

2. Tello, M., C. Lopez-Martinez, and J. J. Mallorqui, "A novel algorithm for ship detection in SAR imagery based on the wavelet transform," *IEEE Geoscience and Remote Sensing Letters*, Vol. 2, No. 2, 201–205, 2005.
3. Farhat, N. H., "Microwave diversity imaging and automated target identification based on models of neural networks," *IEEE Proceedings*, Vol. 77, No. 5, 670–681, 1989.
4. Moon, T. K. and W. C. Stirling, *Mathematical Methods and Algorithms for Signal Processing*, Prentice Hall, 2000.
5. Duda, R. O., P. E. Hart, and D. G. Stork, *Pattern Classification*, 2nd edition, John Wiley & Sons Inc., 2001.
6. Lee, K. C., J. S. Ou, and C. H. Huang, "Angular-diversity radar recognition of ships by transformation based approaches — including noise effects," *Progress In Electromagnetics Research*, PIER 72, 145–158, 2007.
7. Jensen, S. H., P. C. Hansen, S. D. Hansen, and J. A. Sorensen, "Reduction of broad-band noise in speech by truncated QSVD," *IEEE Transactions on Speech and Audio Processing*, Vol. 3, 439–448, 1995.
8. Hermus, K., I. Dologlou, P. Wambacq, and D. V. Compernolle, "Fully adaptive svd-based noise removal for robust speech recognition," *European Conference on Speech Communication and Technology*, 1951–1954, 1999.
9. Konstantinides, K., B. Natarajan, and G. S. Yovanof, "Noise estimation and filtering using blockbased singular value decomposition," *IEEE Transactions on Image Processing*, Vol. 6, 479–483, 1997.
10. Ruck, G. T., D. E. Barrick, W. D. Stuart, and C. K. Krichbaum, *Radar Cross Section Handbook*, Vol. 1, Plenum, New York, 1970.
11. Cui, B., J. Zhang, and X. W. Sun, "Single layer microstrip antenna arrays applied in millimeter-wave radar front-end," *Journal of Electromagnetic Waves and Applications*, Vol. 22, No. 1, 3–15, 2008.
12. Xue W. and X. W. Sun, "Target detection of vehicle volume detecting radar based on Wigner-Hough transform," *Journal of Electromagnetic Waves and Applications*, Vol. 21, No. 11, 1513–1523, 2007.
13. Wang, C. J., B. Y. Wen, Z. G. Ma, W. D. Yan, and X. J. Huang, "Measurement of river surface currents with UHF FMCW radar systems," *Journal of Electromagnetic Waves and Applications*, Vol. 21, No. 3, 375–386, 2007.

14. Jung, J. H., H. T. Kim, and K. T. Kim, "Comparisons of four feature extraction approaches based on Fisher's linear discriminant criterion in radar target recognition," *Journal of Electromagnetic Waves and Applications*, Vol. 21, No. 2, 251–265, 2007.
15. Wang, S. G., X. P. Guan, X. Y. Ma, D. W. Wang, and Y. Su, "Calculating the poles of complex radar targets," *Journal of Electromagnetic Waves and Applications*, Vol. 20, No. 14, 2065–2076.
16. Alivizatos, E. G., M. N. Petsios, and N. K. Uzunoglu, "Towards a range-doppler UHF multistatic radar for the detection of non-cooperative targets with low RCS," *Journal of Electromagnetic Waves and Applications*, Vol. 19, No. 15, 2015–2031, 2005.
17. Capineri, L., D. Daniels, P. Falorni, O. Lopera, and C. Windsor, "Estimation of relative permittivity of shallow soils by using the ground penetrating radar response from different buried targets," *Progress In Electromagnetics Research Letters*, Vol. 2, 63–71, 2008.
18. Abdelaziz, A. A., "Improving the performance of an antenna array by using radar absorbing cover," *Progress In Electromagnetics Research Letters*, Vol. 1, 129–138, 2008.
19. Razevig, V. V., S. I. Ivashov, A. P. Sheyko, I. A. Vasilyev, and A. V. Zhuravlev, "An example of holographic radar using at restoration works of historical building," *Progress In Electromagnetics Research Letters*, Vol. 1, 173–179, 2008.
20. Hebeish, A. A., M. A. Elgamel, R. A. Abdelhady, and A. A. Abdelaziz, "Factors affecting the performance of the radar absorbant textile materials of different types and structus," *Progress In Electromagnetics Research B*, Vol. 3, 219–226, 2008.
21. Chan, Y. K. and V. C. Koo, "An introduction to synthetic aperture radar (SAR)," *Progress In Electromagnetics Research B*, Vol. 2, 27–60, 2008.